THE INTERNATIONAL JOURNAL OF SCIENCE & TECHNOLEDGE

Selection of Shunting Resistance for Cell Equalization in Battery Management System

Hsiang-Fu Yuan
Ph.D. Candidate, SoCLab, Institute of Electrical Control Engineering,
National Chiao-Tung University, Hsinchu, Taiwan (R.O.C.)
Lan-Rong Dung
Professor, SoCLab, Department of Electrical and Computer Engineering,
National Chiao-Tung University, Hsinchu, Taiwan (R.O.C.)

Abstract:
Dissipative shunting resistor is a cheap, simple, and well-known equalizing method for resolving cell mismatch and voltage imbalance problems in a series-connected battery pack. However, seldom information reveals how to choose a good shunting resistance value for the resistor-based equalizer. Determining resistance value based on power dissipation or total equalization time alone is not an attractive solution because a trade-off exists between the two performances. In this paper, energy-time product (ETP) is proposed to be the figure-of-merit for determining the shunting resistance value. The ETP takes both power and time into account, and determines the resistance value by minimizing the ETP value. The first-order battery electrical model is applied to derive the relation between the shunting resistance and ETP, and construct a general way to quickly find the good resistance value. A resistor-based equalizer is implemented to validate the ETP equalizing results and confirms the usefulness of the proposed method. The simulation and experiment results show that the ETP error can be as low as 8.5%.

Keywords: *Lithium-ion battery, Charging equalization, Passive balancing, Shunting resistor.*

1. Introduction

Nowadays, series-connected lithium-ion battery packs have been widely used for electric vehicles (EVs) and hybrid electric vehicles (HEVs). A typical battery pack requires more than 200 Li-ion cells connected in series to fulfill these high voltage demands. However, Li-ion cells are not all identical because of manufacturing variations in nominal charge capacities, internal resistances, and self-discharge rates. The cell mismatch problem causes voltage imbalance during constant-current (CC) charging regimes. As a result, battery packs suffer from overcharging or undercharging phenomena if they do not have any proper protections. This accelerates battery deteriorations (Kuhn, Pitel, & Krein, 2005). In worst case, there is a risk of explosion (Lukic, Cao, Bansal, Rodriguez, & Emadi, 2008). If battery packs have appropriately cell protection mechanisms, the CC charging regime terminates early and brings up another problem: most of fresh cells do not have enough charge capacity during the charging time. To resolve the cell mismatch problem, charging equalization is an essential function for battery management systems (BMS).

Various equalization techniques have been developed in two decades, and well summarized in (Cao, Schofield, & Emadi, 2008; Daowd, Omar, Van Den Bossche, & Van Mierlo, 2011). These techniques can be classified into two categories: dissipative and non-dissipative methods. The dissipative methods bleed excess energy from aging cells using power devices, such as resistor-based (Lindemark, 1991; Stuart & Wei, 2009) and switch-based (Shibata et al., 2001; Teofilo, Merritt, & Hollandsworth, 1997; Uno, 2009). The advantages of this technique are low cost and simple to implementation. However, energy consumption and heat dissipation are major concerns. The non-dissipative methods are developed to improve energy efficiency, and can be further divided into three sub-categories: capacitor-based (Baughman & Ferdowsi, 2008; Kimball, Kuhn, & Krein, 2007; Pascual & Krein, 1997; Uno & Kukita, 2014), inductor-based (Chin-Sien, Kong-Soon, & Jin-Shin, 2009; Kutkut, 1998; Mestrallet, Kerachev, Crebier, & Collet, 2014; Uno & Tanaka, 2013), and transformer-based equalization approaches (Einhorn, Roessler, & Fleig, 2011; Hong-sun, Chong-Eun, Chol-Ho, Gun-Woo, & Joong-Hui, 2009; Hung, Hopkins, & Mosling, 1993; Kutkut, Wiegman, Divan, & Novotny, 1999). These techniques transfer excess energy from aging cells to fresh cells, from the entire battery pack to fresh cells, or from aging cells to the entire battery pack (Andrea, 2010; Moon-Young, Jun-Ho, & Gun-Woo, 2014). Despite successfully decreasing the energy consumption, high cost is the main disadvantage.

This paper focuses on the dissipative shunting resistor-based equalizer. This method utilizes shunting resistors across aging cells in a pack to bleed excess energy, and waits for fresh cells to catch up. However, little research provides a selection guide to determine a proper resistance value. The shunting resistance value can greatly affect the equalization time and power dissipation. Both of them are important equalizing performances, but a trade-off exists between the two performances. This situation usually causes some confusion for the BMS designers who need to choose a good resistance value in their equalizers.

In this paper, energy-time product (ETP) is proposed to be the figure-of-merit for determining the shunting resistance value. The concept of ETP comes from the merit of energy-delay product (EDP) (Gonzalez & Horowitz, 1996; Horowitz, Indermaur, & Gonzalez, 1994), which has been used to assess the performances of a microprocessor because a trade-off between power and gate delay exists in low-power digital circuit design. The first-order battery electrical model is applied to model the resistor-based equalizers and to construct a general way to quickly determine the good resistance value by minimizing the ETP value. An equalizer implemented with a 3S1P $LiCoO_2$ batter pack confirms the usefulness of the proposed approach. The simulation and experiment results show that the ETP error can be as low as 8.5%.

This paper is organized as follows: Section 2 introduces the shunting resistor-based equalizer. In Section 3, the proposed merit of ETP is addressed, and the relation to the resistance value is also derived using the first-order battery model. Section 4 shows the implementation of the equalizer for validation tests. Section 5 presents experimental results and the final conclusion is given in Section 6.

2. Dissipative Shunting Resistor-Based Equalizer

2.1. Circuit Topology

Fig. 1 shows the circuit topology of the dissipative shunting resistor-based equalizer. Every battery cell (B) connects a power switch (S) and a shunting resistor (R_{sh}) in parallel to bleed excess energy if necessary. For N battery cells, the equalizer has N power switches and N shunting resistors. Voltage sensors with level shifters are required to measure and send the cell voltages (V_b) to the analog-to-digital (ADC) converter. Microcontroller controls the gate drivers (G_b) of the power switches, and determines whether to turn on them or not.

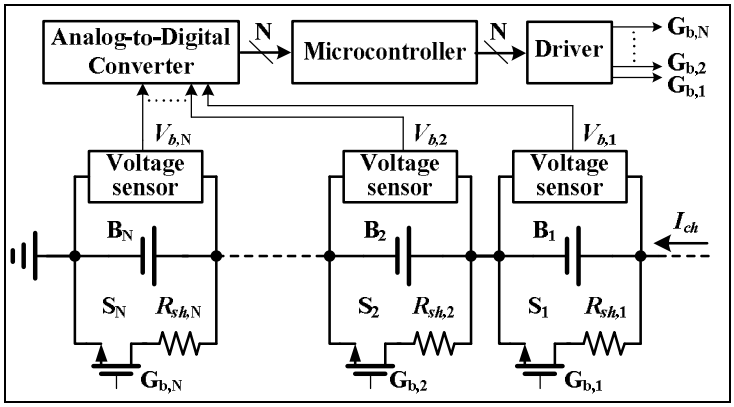

Figure 1: Circuit topology of a dissipative shunting resistor-based equalizer

2.2. Operation Principle

The operation principle of the shunting resistor-based equalizer is sample as shown in Fig. 2. When charging starts, all cell voltages rise. Equalization is only triggered if any cell voltage hits the overvoltage threshold (V_{ov}). Normally, the aging cells in a battery pack have a high chance to reach this threshold firstly, because the growing impedances cause them higher charging voltages then the fresh cell voltages. In equalization mode, charging is halted and the shunting resistor starts to discharge the cell that reaches the V_{ov} limit. When the cell voltage drops to the recovery limit, V_{ov} - ΔV_{ovh}, the battery pack recharges until any cell hits the V_{ov} limit again. The ΔV_{ovh} is the overvoltage detection hysteresis. After numerous equalization/recharging cycles, the voltage imbalance can be effectively shrunk as shown in Fig. 2. The original voltage difference, ΔV_i, reduces to ΔV_e at the end of charging.

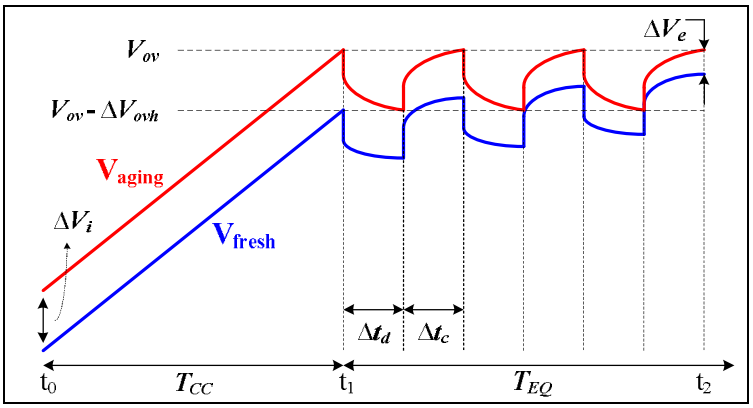

Figure 2: Illustration of operation principle

2.3. Performance

Equalization time and power dissipation are two major performances that we are mostly concerned. Power dissipation has the influence on the size of the equalizer circuit. High power dissipation increases not only the volume of the equalizer circuit but also the difficulty to manage thermal problems. Equalization time determines the total charging time. A long equalization time is not always accepted by numerous EV users. Unfortunately, the shunting resistor-based equalizer cannot possess good performances on power dissipation and equalization time simultaneously. There is a trade-off between them. For example, a small shunting resistance value enhances the bleeding current and shortens the equalization time, but also leads to high power dissipation. Therefore, a major question is how to select an appropriate shunting resistance value, and how to assess the real performance of the resistor-based equalizer.

3. Energy-Time Product

In this paper, energy-time product is proposed to be a selection guide for the shunting resistance value. The ETP is a figure-of-merit that takes both power dissipation and equalization time into account, and is expressed as Eq. (1).

ETP = power dissipation $\times$ equalization time^2 (1)

The weighting of equalization time is 2, so that the product is able to truly reflect the performance of a resistor-based equalizer. The shunting resistance value can be determined by minimizing the merit of ETP. To derive the relation between ETP and the shunting resistance value, the first-order battery electrical model is used to model the equalizer.

3.1. Battery Model

A battery can be equivalent to a first-order battery electrical model in Fig. 3. The battery model is developed based on Thevenin's theorem and consists of three major components including a dependent voltage source, a RC parallel circuit, and an ohmic resistance. The dependent voltage source represents battery electromotive force (EMF), which is an open-circuit voltage (OCV) when the battery has a long rest time for full relaxation. The RC parallel circuit (R_p//C_p) is composed of a transient resistance and a transient capacitance for modeling battery transient behaviors, such as kinetic and diffusion reactions. The ohmic resistance (R_s) is the pure resistances in two electrodes, electrolyte, and separator. The ohmic resistance describes the instantaneous voltage change when the battery has a step current.

All these battery model parameters are function of the battery state-of-charge (SOC), which is used to indicate the remaining useful charge inside a battery. A well-known technique to know the battery SOC information is coulomb counter. This technique estimates battery SOCs based on current integration as expressed in Eq. (2).

$$\mathrm{SOC}(t) = \mathrm{SOC}(t_0) + \frac{\int I_b(t)dt}{Q_{nom}} \cdot 100\% \quad (2)$$

where I_b is the battery current, and is positive during charging periods or negative during discharging periods. The Q_{nom} is the battery nominal capacity claimed by manufacturer. With coulomb counter, the battery SOC is easy to trace and applied to further analyze the performances of the equalizer.

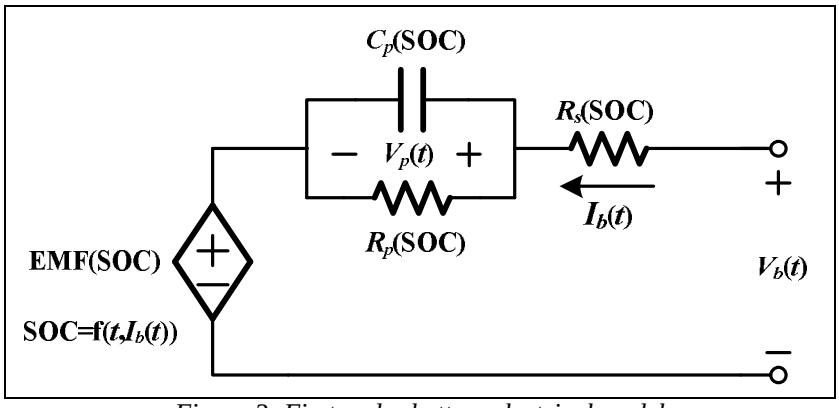

Figure 3: First-order battery electrical model

3.2. Maximum Power Dissipation

By replacing battery cells with the first-order electrical model, the equivalent circuit of the resistor-based equalizer is demonstrated in Fig. 4. In equalization model, the charger is turned off temporarily, so the bleeding current is only depended on two factors: EMF and the voltage across the transient capacitance (V_p). Based on the superposition law, the respective currents are derived as Eq. (3)-(5).

$$I_{sh1}(t) = \mathrm{EMF} \cdot \left[\frac{1}{R_k + R_p} + \frac{R_p}{R_k (R_k + R_p)} e^{-\alpha t} \right] \tag{3}$$

$$I_{sh2}(t) = \frac{V_p}{R_k} e^{-\alpha t} \tag{4}$$

$$\alpha = -\frac{R_k + R_p}{R_k R_p C_p} \tag{5}$$

where $I_{sh1}(t)$ is the current of EMF, $I_{sh2}(t)$ is the current of V_p, and R_k is R_s+R_{sh}. Due to the flat voltage curve of Li-ion batteries, the change of EMF value is negligible and can be ignored. The bleeding current is the sum of Eq. (3) and Eq. (4).

$$I_{sh}(t) = \frac{\mathrm{EMF}}{R_k + R_p} + \left[\frac{\mathrm{EMF} \cdot R_p}{R_k (R_k + R_p)} + \frac{V_p}{R_k} \right] e^{-\alpha t} \tag{6}$$

Obviously, a small shunting resistor will lead to a high bleeding current. In addition, the bleeding current decays exponentially with time, so the maximum current and power dissipation happen at the beginning of equalization mode. The maximum power dissipation is described in Eq. (7).

$$\begin{aligned} P_{\max} &= \left[I_{sh}(t=0) \right]^2 \cdot R_{sh} \\ &= \frac{R_{sh}}{R_k^{\,2}} \left(\mathrm{EMF} + V_p \right)^2 \end{aligned} \tag{7}$$

where the maximum value is strongly correlated with the EMF and initial capacitance voltage values in equalization mode.

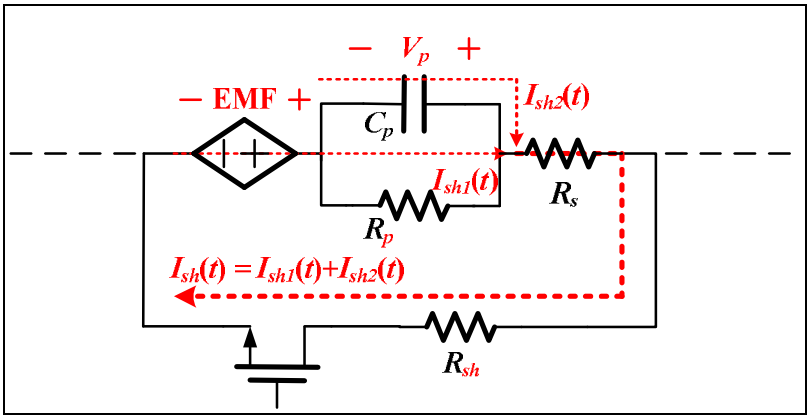

Figure 4: Equivalent circuit of the resistor-based equalizer for maximum power analysis

3.3. Total Equalization Time

Resistor-based equalizers balance a battery pack with a series of charging/discharging cycles. In each charging/discharging cycle, battery voltage imbalance reduces gradually. A battery pack is well-equalized when the imbalance level decreases to the preset range, such as the ΔV_{ovh} in Fig. 2. Based on the operation principle, the total equalization time can be expressed as Eq. (8).

$$T_{EQ} = M \cdot (\Delta t_c + \Delta t_d) \tag{8}$$

where T_{EQ} is the total equalization time, Δt_c and Δt_d are the charging and discharging times in equalization mode, and M is the required equalization cycles. The M is defined as Eq. (9).

$$M = \frac{\Delta Q_i - \Delta Q_e}{\Delta Q_c} \tag{9}$$

where ΔQ_i and ΔQ_e are the charge capacity differences between the aging and fresh cells in the initial and final cycles, and ΔQ_c is the increment charge of the battery pack in the charging time Δt_c. The ΔQ_i -ΔQ_e term is the remaining charge needed to be reduced in the consecutive charging/discharging cycles. Substituting equation Eq. (9) into Eq. (8) and replacing ΔQ_c with $I_{ch} \cdot \Delta t_c$, the total equalization time is deduced to another form in Eq. (10).

$$T_{EQ} = \frac{\Delta Q_i - \Delta Q_e}{I_{ch}} \cdot \left(1 + \frac{\Delta t_d}{\Delta t_c}\right) \tag{10}$$

The term outside brackets is only depended on the current level in the CC charging regime, battery initial conditions, and the equalization target. The term of $(1+\Delta t_d / \Delta t_c)$ is the main factor to determine the length of the total equalization time, and we call it equalization time factor (TF_e). In the charging/discharging cycles, the aging cell is charged and discharged with the same charge, so the time ratio in the TF_e equation can be further simplified to an average current ratio.

$$\mathrm{TF_e} = 1 + \frac{I_{c,avg}}{I_{d,avg}} \tag{11}$$

where

$$I_{c,avg} = I_{ch} \tag{12}$$

$$I_{d,avg} = \frac{\mathrm{EMF} + V_p}{R_k} - \frac{1}{2} \cdot \alpha \cdot \left[\frac{\mathrm{EMF}}{R_k (R_k + R_p)} + \frac{V_p}{R_k} \right] \cdot \Delta t_d \tag{13}$$

$$\Delta t_d = -\frac{1}{\alpha} \cdot \ln(1 - X) \tag{14}$$

$$X = \left[\Delta V_{ovh} - \left(I_{ch} + \frac{\mathrm{EMF} + V_p}{R_k} \right) \cdot R_s \right] \cdot \left[\left(\frac{\mathrm{EMF}}{R_k (R_k + R_p)} + \frac{V_p}{R_k} \right) \cdot R_{sh} \right]^{-1} \tag{15}$$

The relation between the shunting resistance and TF_e is constructed to realize the effect of shunting resistance on the equalization time. In Eq. (11), a small shunting resistance can increase the average bleeding current in the discharging cycle, reduce TF_e value, and shorten the equalization time.

3.4. Resistance Value Determination based on ETP

The shunting resistance value with the minimum ETP is proposed in this paper to equalize an imbalance battery pack. To find this resistance value, the minimum ETP is searched by optimizing the product of the maximum power dissipation and the square of TF_e.

$$R_{sh} = \min\left(P_{\max} \cdot \mathrm{TF_e}^2\right) \tag{16}$$

In this case, the extreme value theorem is a useful tool to solve this problem.

4. Implementation

A resistor-based equalizer with a 3S1P battery pack is implemented in Fig. 5 to validate the equalizing results of ETP. The battery cells used in this test are the commercial off-the-shelf $LiCoO_2$ batteries with the 1.1Ah nominal charge capacity. Three cells have different aging deteriorations: 200 cycles, 50 cycles, and 10 cycles for B_1, B_2, and B_3 cells. Because the aging cell, B_1, will reach the V_{ov} threshold firstly, various shunting resistance values are parallel-connected with it to test the equalizing performances including maximum power dissipation, TF_e, and ETP. The difference amplifiers connected with unity-gain voltage buffers are the voltage sensors to extract each cell voltage. The TLP250 photocoupler is used to be the gate drivers for switching the IRFZ34N power MOS. The battery cells, shunting resistances, voltage sensors, and gate drivers are all implemented in the equalizer board in Fig. 5(a).

The experimental setup of the charging equalization experiments is shown in Fig. 5(b). A GW Instek PSM-2010 programmable and single channel DC power supply is used as the battery charger. A Chroma 63010 DC electronics load provides a discharge current for testing the battery pack. A multifunction data acquisition card, NI USB-6009, measures cell voltages that are delivered from the voltage sensors, and sends the control signals to relays and power MOS switches. A personal computer integrates all instruments and performs the equalization algorithm that is coded in LabVIEW programming environment. The flow chart of the control algorithm is shown in Fig. 6. In this algorithm, the operations are divided into CC charging mode, equalization mode, and discharging mode.

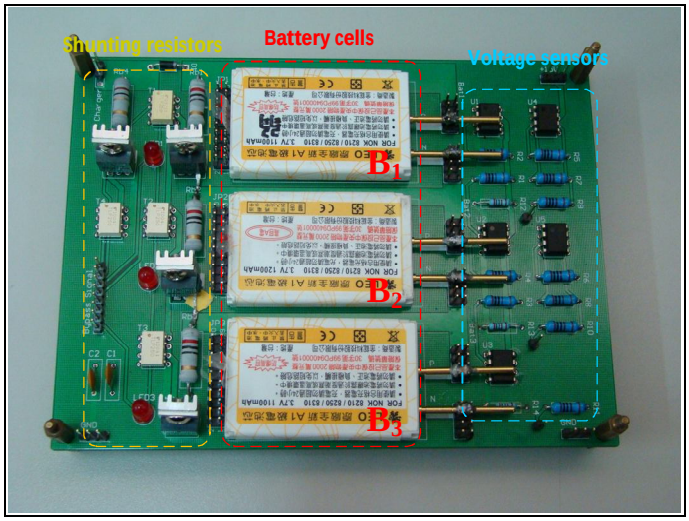

(a)

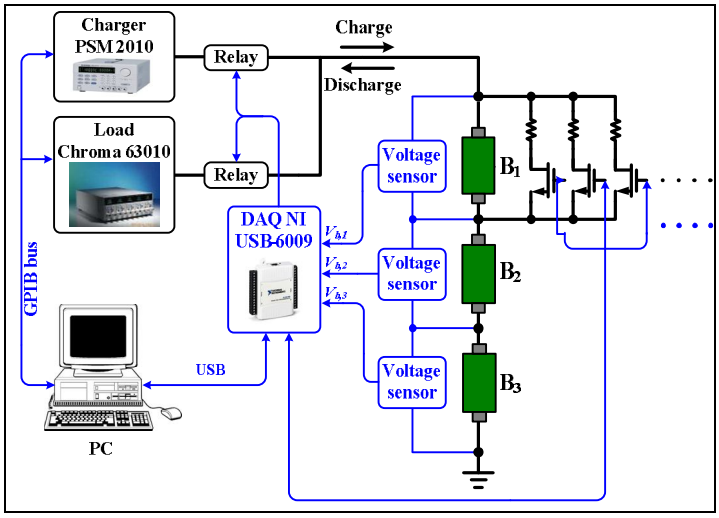

(b)

Figure 5: Implementation of the resistor-based equalizer with a 3S1P battery pack (a) Equalizer board (b) Experimental setup

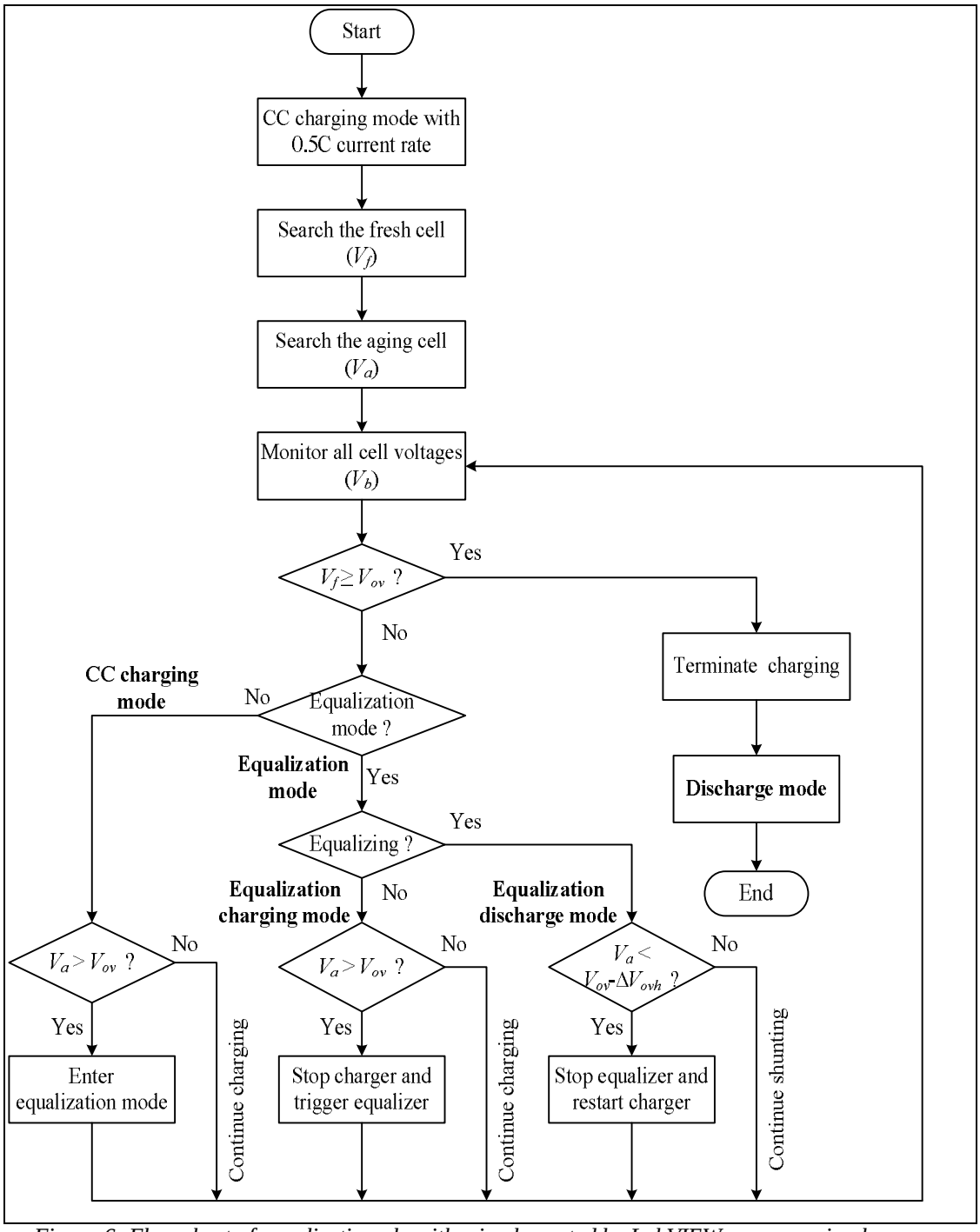

Figure 6: Flow chart of equalization algorithm implemented by LabVIEW programming language

5. Experimental Results

The experimental results of 10Ω shunting resistance is presented in Fig. 7. In this test, the CC charging current is 0.5C or 550mA, the V_{ov} threshold is 4.22V, and the ΔV_{ovh} is 0.22V. The whole charging time (T_{CC}+T_{EQ}) is almost 5.1hrs. The CC charging time (T_{CC}) is only 0.6hr, and the total equalization time (T_{EQ}) is 4.95hrs, which is 97% of the total charging time. Moreover, the maximum bleeding current is about 410mA and generates the maximum 1.68W power dissipation.

The distributions of cell voltages before and after equalization are compared in Fig. 7(b). Before equalization, the total pack voltage is 11.502V. Among them, the aging cell, B_1, has the highest voltage level, 4.097V, and the fresh cell, B_2, has the lowest voltage level, 3.7V. The voltage difference between the two cells is 0.397V. After equalization, the battery pack is successfully balanced by decreasing 87% of the original voltage difference from 0.397V to 0.053V. The voltage difference at the end of equalization satisfies the goal. In addition, the total pack voltage also increases to 12.122V.

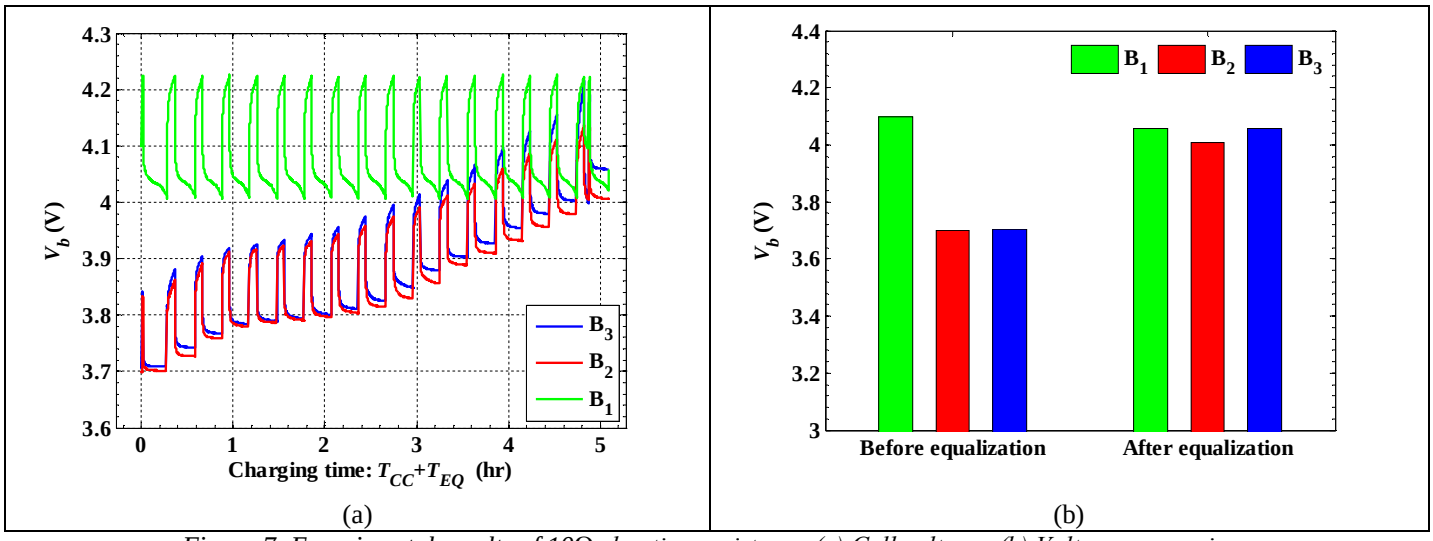

Figure 7: Experimental results of 10Ω shunting resistance (a) Cell voltages (b) Voltage comparison

Fig. 8 shows the validation results of the equalizing performances. Comparisons were made between simulation and experiment data. The simulation data comes from the equations derived in section 3. The experiment data were tested repeatedly with various resistance values ranged from 2.5Ω to 50Ω. Fig. 8(a)-(c) are the comparison results of power, TF_e, and ETP respectively. In Fig. 8(a), the simulation and experiment results show the consistency in the power trend. The power trend exponentially decreases with the increasing resistance value. In Fig. 8(b), the TF_e comparison also has a good agreement. Both results show a linearly growing trend with the shunting resistance. In Fig. 8(c), the simulation results show that ETP has the minimum value in the range of 4.9Ω to 5.8Ω resistance value, and the minimum product of $P_{max} \cdot TF_e^{\ 2}$ is about 8.214W. The experiment result of 5Ω resistance value validates that ETP has the minimum value in this range, and the product of $P_{max} \cdot TF_e^{\ 2}$ is 7.566W. The ETP error between the simulation and experiment results is only 8.5%.

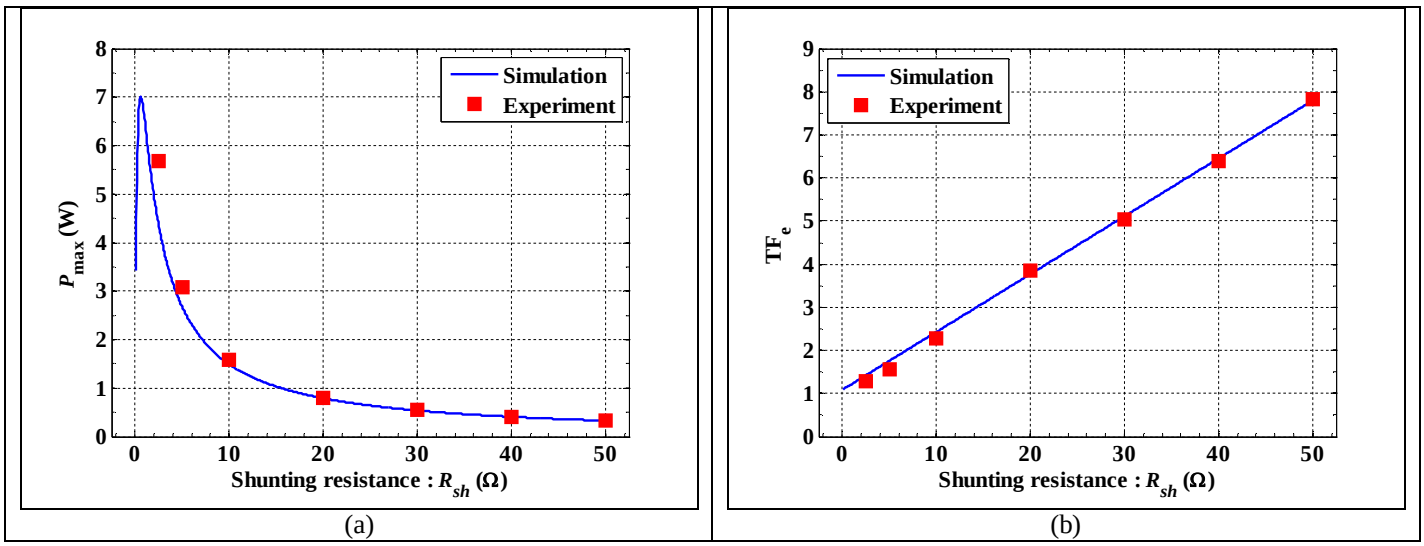

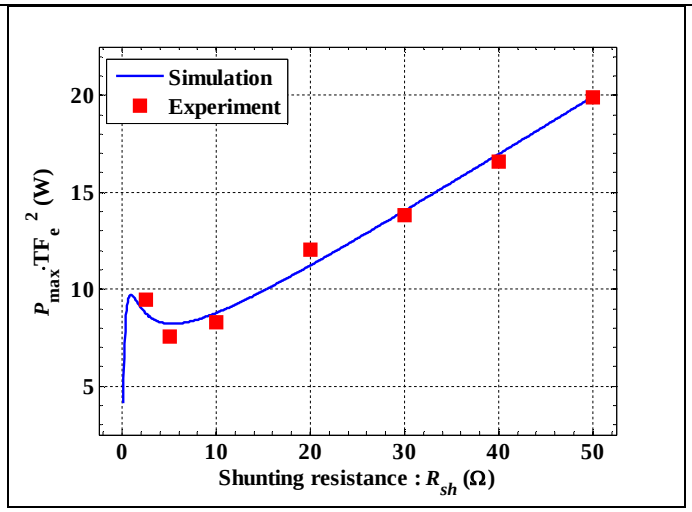

(c)

Figure 8: Equalizing performance validation (a) Maximum power dissipation (b) TF_e (c) ETP

6. Conclusion

Due to the trade-off between the power dissipation and the equalization time, the merit of ETP is proposed in this paper to be the selection guide for shunting resistance value determination. The first-order battery electrical model is applied to derive the relations between the shunting resistance value, the maximum power dissipation, and the total equalization time. The shunting resistance value is determined by searching the minimum ETP value, and this is achieved by optimizing the product of maximum power dissipation and the square of TF_e. A resistor-based equalizer with a 3S1P $LiCoO_2$ battery pack is implemented to validate the ETP equalizing results. The validation tests confirm the usefulness of the proposed approach to resistance value determination. The simulation and experiment results show that the ETP error can be as low as 8.5%.

7. References

i. Andrea, D. (2010). Battery Management Systems for Large Lithium Ion Battery Packs: Artech House.
ii. Baughman, A. C., & Ferdowsi, M. (2008). Double-tiered switched-capacitor battery charge equalization technique. IEEE Trans. Ind. Electron., 55(6), 2277-2285.
iii. Cao, J., Schofield, N., & Emadi, A. (2008, Sept. 3-5). Battery balancing methods: A comprehensive review. Paper presented at the Proc. IEEE Veh. Power Propulsion Conf. (VPPC).
iv. Chin-Sien, M., Kong-Soon, N., & Jin-Shin, H. (2009, Feb. 10-13). Operation of battery power modules with series output. Paper presented at the Proc. IEEE Int. Conf. Industrial Technology, Gippsland, VIC.
v. Daowd, M., Omar, N., Van Den Bossche, P., & Van Mierlo, J. (2011, Sept. 6-9). Passive and active battery balancing comparison based on MATLAB simulation. Paper presented at the Proc. IEEE Veh. Power Propulsion Conf. (VPPC), Chicago, IL.
vi. Einhorn, M., Roessler, W., & Fleig, J. (2011). Improved performance of serially connected Li-ion batteries with active cell balancing in electric vehicles. IEEE Trans. Veh. Technol., 60(6), 2448-2457.
vii. Gonzalez, R., & Horowitz, M. (1996). Energy dissipation in general purpose microprocessors. IEEE J. Solid-State Circuits, 31(9), 1277-1284.
viii. Hong-sun, P., Chong-Eun, K., Chol-Ho, K., Gun-Woo, M., & Joong-Hui, L. (2009). A modularized charge equalizer for an HEV lithium-ion battery string. IEEE Trans. Ind. Electron., 56(5), 1464-1476.
ix. Horowitz, M., Indermaur, T., & Gonzalez, R. (1994, Oct. 10-12). Low-power digital design. Paper presented at the Proc. IEEE Symp. Low-Power Electron., San Diego, CA (USA).
x. Hung, S. T., Hopkins, D. C., & Mosling, C. R. (1993). Extension of battery life via charge equalization control. IEEE Trans. Ind. Electron., 40(1), 96-104.
xi. Kimball, J. W., Kuhn, B. T., & Krein, P. T. (2007, Sept. 9-12). Increased performance of battery packs by active equalization. Paper presented at the Proc. IEEE Veh. Power Propulsion Conf. (VPPC), Arlington, TX.
xii. Kuhn, B. T., Pitel, G. E., & Krein, P. T. (2005, Sept. 7-9). Electrical properties and equalization of lithium-ion cells in automotive applications. Paper presented at the Proc. IEEE Veh. Power Propulsion Conf. (VPPC), Chicago, IL.
xiii. Kutkut, N. H. (1998, Feb. 15-19). A modular nondissipative current diverter for EV battery charge equalization. Paper presented at the Proc. 13th IEEE Appl. Power Electron. Conf. Expo., Anaheim, CA.
xiv. Kutkut, N. H., Wiegman, H. L. N., Divan, D. M., & Novotny, D. W. (1999). Design considerations for charge equalization of an electric vehicle battery system. IEEE Trans. Ind. Appl., 35(1), 28-35.
xv. Lindemark, B. (1991, Nov. 5-8). Individual cell voltage equalizers (ICE) for reliable battery performance. Paper presented at the Proc. 13th Annu. Int. Telecommun. Energy Conf. (INTELEC), Koyto, Japan.

xvi. Lukic, S. M., Cao, J., Bansal, R. C., Rodriguez, F., & Emadi, A. (2008). Energy storage systems for automotive applications. IEEE Trans. Ind. Electron., 55(6), 2258-2267.

xvii. Mestrallet, F., Kerachev, L., Crebier, J. C., & Collet, A. (2014). Multiphase interleaved converter for lithium battery active balancing. IEEE Trans. Power Electron., 29(6), 2874-2881.

xviii. Moon-Young, K., Jun-Ho, K., & Gun-Woo, M. (2014). Center-cell concentration structure of a cell-to-cell balancing circuit with a reduced number of switches. IEEE Trans. Power Electron., 29(10), 5285-5297.

xix. Pascual, C., & Krein, P. T. (1997, Feb. 23-27). Switched capacitor system for automatic series battery equalization. Paper presented at the Proc. 12th IEEE Appl. Power Electron. Conf. Expo., Atlanta, GA.

xx. Shibata, H., Taniguchi, S., Adachi, K., Yamasaki, K., Ariyoshi, G., Kawata, K., et al. (2001, Oct. 22-25). Management of serially-connected battery system using multiple switches. Paper presented at the Proc. 4th IEEE Int. Conf. Power Electron. Drive Syst.

xxi. Stuart, T. A., & Wei, Z. (2009). Fast equalization for large lithium ion batteries. IEEE Aerosp. Electron. Syst. Mag., 24(7), 27-31.

xxii. Teofilo, V. L., Merritt, L. V., & Hollandsworth, R. P. (1997). Advanced lithium ion battery charger. IEEE Aerosp. Electron. Syst. Mag., 12(11), 30-36.

xxiii. Uno, M. (2009, Oct. 18-22). Interactive charging performance of a series connected battery with shunting equalizers. Paper presented at the Proc. 31st Annu. Int. Telecommun. Energy Conf. (INTELEC), Incheon, South Korea.

xxiv. Uno, M., & Kukita, A. (2014). Double-switch equalizer using parallel- or series-parallel-resonant inverter and voltage multiplier for series-connected supercapacitors. IEEE Trans. Power Electron., 29(2), 812-828.

xxv. Uno, M., & Tanaka, K. (2013). Single-switch multioutput charger using voltage multiplier for series-connected lithium-ion battery/supercapacitor equalization. IEEE Trans. Ind. Electron., 60(8), 3227-3239.